Elastic local buckling of thin-walled elliptical tubes containing elastic infill material

M.A. Bradford[†] and A. Roufegarinejad[‡]

*Centre for Infrastructure Engineering and Safety, School of Civil and Environmental Engineering
The University of New South Wales, Sydney, NSW 2052, Australia*

Abstract.   Elliptical tubes may buckle in an elastic local buckling failure mode under uniform compression. Previous analyses of the local buckling of these members have assumed that the cross-section is hollow, but it is well-known that the local buckling capacity of thin-walled closed sections may be increased by filling them with a rigid medium such as concrete. In many applications, the medium many not necessarily be rigid, and the infill can be considered to be an elastic material which interacts with the buckling of the elliptical tube that surrounds it. This paper uses an energy-based technique to model the buckling of a thin-walled elliptical tube containing an elastic infill, which elucidates the physics of the buckling phenomenon from an engineering mechanics basis, in deference to a less generic finite element approach to the buckling problem. It makes use of the observation that the local buckling in an elliptical tube is localised with respect to the contour of the ellipse in its cross-section, with the localisation being at the region of lowest curvature. The formulation in the paper is algebraic and it leads to solutions that can be determined by implementing simple numerical solution techniques. A further extension of this formulation to a stiffness approach with multiple degrees of buckling freedom is described, and it is shown that using the simple one degree of freedom representation is sufficiently accurate for determining the elastic local buckling coefficient.

Keywords: elastic buckling; elastic restraint; ellipse; local buckling; localisation; Ritz technique.

1. Introduction

   Thin-walled circular tubes subjected to axial compression find widespread application in many branches of engineering, and their buckling behaviour has been researched fairly extensively. On the other hand, the structural behaviour and particularly the buckling response of elliptical tubes has been far less studied, despite their growing use in engineering structures and related applications, especially in stainless steel and advanced composite materials (Bortolotti *et al.* 2003, Mahdi *et al.* 2005, Chan and Gardner 2006, Gardner and Chan 2006, Zhu and Wilkinson 2006). While it is widely known that imperfection sensitivity is dominant in the buckling of thin-walled circular tubes and leads to sudden failures which must be analysed by Donnell shell theory or the like (Teng 1996), the buckling of elliptical tubes is less explosive insofar as failure may occur beyond the initial buckling load and the postbuckling range is not necessarily accompanied by rapid strain softening (Hutchinson 1968).
   It is also well-known, in practical applications in structural engineering, that the strength enhancement

† Professor, Corresponding Author, E-mail: m.bradford@unsw.edu.au
‡ Research Student

of infilling a hollow steel tube with concrete arises not only because of the inclusion of the strength of the concrete infill itself, but because it also increases the local buckling capacity of the encasing tube by inhibiting the buckling of the tube into the infill (Uy 2001). This latter effect was considered for circular tubes by Bradford *et al.* (2002), who derived an analytical expression for the local buckling of a thin-walled circular tube with a rigid infill in closed form. More generally, hollow tubes, and tubes with an infinitely stiff (or rigid) infill, represent two extremes of a restraint condition, in which an elastic infill of quantifiable stiffness may interact with the infinitesimal buckling deformations that accompany bifurcative local buckling of a thin-walled tube. This possibility of the infill being elastic rather than rigid, and its influence on buckling, was considered by Bradford and Vrcelj (2004) for square tubes and by Bradford and Roufegarinejad (2006) and Bradford *et al.* (2006) for circular tubes. Related applications for circular tubes are suction caissons (Pinna and Ronalds 2000) where the soil provides elastic restraint at the level of the seabed, as well as in crashworthiness applications (Reddy and Wall 1988, Guillow *et al.* 2001) and the seismic design of buckling restrained braces (Black *et al.* 2004). Hitherto, it appears the influence of an elastic infill (and even a rigid infill of infinite stiffness) on the buckling of thin-walled elliptical tubes has not been reported. This paper therefore considers the buckling of a thin-walled elliptical tube, in which a prebuckling plane stress state (and with flexure caused by local buckling) in a scale of the order of the thickness of the tube interacts with a plane stress state in the infill of the scale of the order of the tube diameter.

Sustained research outcomes on the stability of elliptical tubes appears to date from the work of Marguerre (1951), who proposed a "mean value" of the curvature of the ellipse as a basis for an equivalent radius of a circular tube, but the use of this concept led to erroneous predictions of the buckling stress. This concept was explored further by Kempner (1962). Kempner's work recognised the 'localisation' of the buckle of an elliptical tube, as shown in Fig. 1, where the buckle is localised in a region $2\beta a$ adjacent to the position in the profile where the curvature is smallest, where a is the semi-major axis of the ellipse and β represents a localisation parameter. This concept is used in the present paper. Several other researchers have addressed the hollow elliptical tube buckling problem, including Tennyson *et al.* (1971),
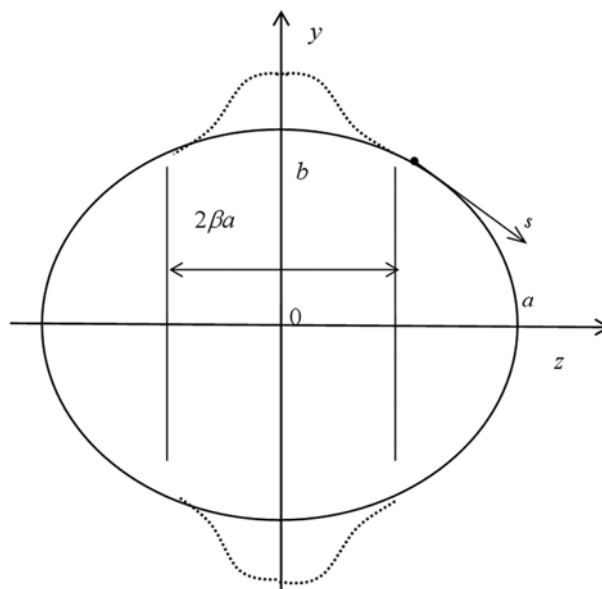

Fig. 1 Localisation of buckling of elliptical tube

Myers and Hyer (1999) and Hyer and Vogl (2001), but research of the topic has been far from extensive.

In this paper, the local buckling of thin-walled elliptical tubes containing an elastic infill under uniform compression is studied theoretically using a generic approach. It is based on a consideration of the similar problem for circular tubes reported elsewhere (Bradford and Roufegarinejad 2006, Bradford *et al.* 2006), with a consideration of the observed localisation of the buckled shape that is peculiar to elliptical tubes in order to simplify the analysis. The problem is stated in analytical form, from which numerical solutions may be derived, and that are compared with finite element results obtained using ABAQUS (2006). The use of a one-degree of freedom formulation for the problem is shown to be accurate when compared with ABAQUS, and with the formulation herein when used with more than one degree of freedom. The use of an approximate solution, again in closed form, is proposed and discussed.

2. Energy formulation for change in potential during buckling

The local buckling mode for an elliptical section shown in Fig. 2 is assumed to be infinitesimal and of magnitude w in the local normal (s) direction, that is produced when a constant uniaxial strain ε_0 applied in the x-direction reaches its critical value ε_{0l} at which elastic bifurcation buckling takes place. One local buckling cell of wavelength L in the x-direction is considered here; this being one of a number of such cells that are assumed to form lengthwise. The energy formulation (Bradford *et al.* 2006) requires statements of the strain energy stored due to bending only (U_b), the membrane strain energy due to stretching (U_m), the strain energy stored in the elastic infill (U_r) as well as the work done during buckling (V).

The middle or reference surface normal and shear strains for the ellipse (where u and v are the axial and circumferential displacements respectively) are
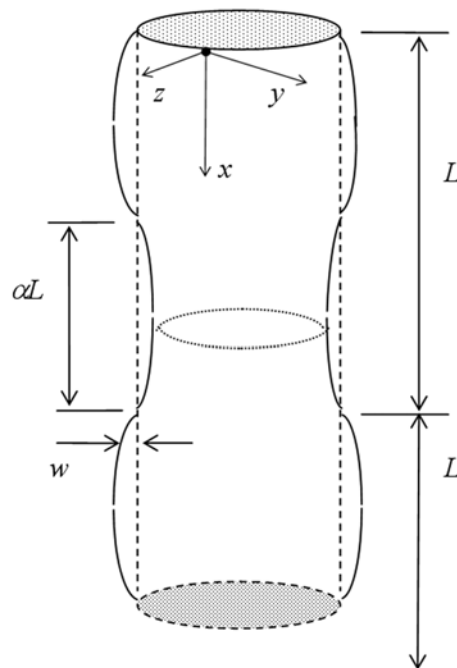

Fig. 2 Axes, buckled shape and buckling wavelength

$$\varepsilon_x = \partial u / \partial x; \ \varepsilon_s = \partial v / \partial s + w / \rho; \ \gamma_{xs} = \partial u / \partial s + \partial v / \partial x \tag{1}$$

while the curvatures are

$$\kappa_x = -\partial^2 w / \partial x^2; \ \kappa_s = -\partial^2 w / \partial s^2; \ \kappa_{xs} = -2 \partial^2 w / \partial x \partial s \tag{2}$$

in which ρ is the local radius of curvature of the undeformed tube that varies around its elliptical profile. The generalised curvatures in Eqs. (1) and (2) lead to the well-known strain energy stored due to bending only as

$$U_b = \frac{D}{2} \int_0^L \oint_C [\kappa_x^2 + \kappa_s^2 - 2(1-\nu)(\kappa_x \kappa_s - \kappa_{xs}^2)] \, ds \, dx \tag{3}$$

in which

$$D = \frac{Et^3}{12(1-\nu^2)} \tag{4}$$

is the stiffness of the tube, E is Young's modulus, ν is Poisson's ratio and C denotes the elliptic contour with the integration $\oint (\ ) ds$ being around this closed contour.

By using elementary elasticity theory (Timoshenko and Goodier 1970), the stresses through the thickness ($z \in [-t/2, t/2]$) corresponding to ε_x and ε_s are

$$\sigma_x(z) = \left(\frac{E}{1-\nu^2}\right)[(\varepsilon_x - z\kappa_s) + \nu(\varepsilon_s - z\kappa_s)] \tag{5}$$

and

$$\sigma_s(z) = \left(\frac{E}{1-\nu^2}\right)[(\varepsilon_x - z\kappa_s) + \nu(\varepsilon_x - z\kappa_x)] \tag{6}$$

which lead to edge forces per unit length of

$$N_x = \int_{-t/2}^{t/2} \sigma_x dz = \frac{Et(\varepsilon_x + \nu\varepsilon_s)}{1-\nu^2} \tag{7}$$

and

$$N_s = \int_{-t/2}^{t/2} \sigma_s dz = \frac{Et(\varepsilon_s + \nu\varepsilon_x)}{1-\nu^2} \tag{8}$$

as well as

$$N_{xs} = \int_{-t/2}^{t/2} \tau_{xs} dz = \frac{Et\gamma_{xs}}{2(1+\nu)} \tag{9}$$

where γ_{xs} is the shear strain at the middle surface of the ellipse. At buckling, the axial force intensity is $(\varepsilon_0 E)t$, which must be equal to N_x in Eq. (7), and which results in

$$\varepsilon_0 = \frac{(\varepsilon_x + \nu\varepsilon_s)}{1-\nu^2} \tag{10}$$

while the strain $-\nu\varepsilon_0$ in the s direction because of Poisson's effect must be augmented by the membrane buckling strain w/ρ, producing

$$\varepsilon_s = \frac{w}{\rho} - \nu\varepsilon_0 \tag{11}$$

Solving Eqs. (10) and (11) simultaneously then leads to

$$\varepsilon_x = \varepsilon_0 - \frac{\nu w}{\rho} \tag{12}$$

During buckling, strain energy is also stored due to membrane stretching, and this is given by

$$U_s = \frac{1}{2}\oint_C \int_{-t/2}^{t/2} (N_x\varepsilon_x + N_s\varepsilon_s + N_{xs}\gamma_{xs})\mathrm{d}z\,\mathrm{d}s \tag{13}$$

and which using Eqs. (7) to (9) results in

$$U_s = \frac{Et}{2(1-\nu^2)}\oint_C \int_{(-t/2)}^{t/2} \left[(\varepsilon_x + \varepsilon_s)^2 - 2(1-\nu)\left(\varepsilon_x\varepsilon_s - \frac{\gamma_{xs}^2}{4}\right) \right]\mathrm{d}z\,\mathrm{d}s \tag{14}$$

During buckling, the end external compressive forces do work that is equal to the end load multiplied by the axial shortening $1/2\int(\partial w/\partial x)^2\mathrm{d}x$ and by the change in axial length caused by the change in strain $\varepsilon_x - \varepsilon_0$ (Eq. 12), so that

$$V = Et\varepsilon_0 \int_0^L \oint_C \left[(\varepsilon_x - \varepsilon_0) + \frac{1}{2}\left(\frac{\partial w}{\partial x}\right)^2 \right]\mathrm{d}s\,\mathrm{d}x \tag{15}$$

Fig. 3 shows a cross-sectional view of a local buckling cell along a meridian, with an interface region between the tube and elastic infill defined by $\Gamma = [0, \alpha L]$. When $x \in \Gamma$, the local buckle in the thin-walled ellipse penetrates the elastic medium which has a constant stiffness k (which has units of force per area per unit length); when $x \notin \Gamma$ the tube buckles away analogous to a plate on a tensionless foundation (Smith *et al.* 1998). For a given local buckle cell length L, the penetration parameter $\alpha \in [0,1]$ defines the extent to which the buckle penetrates the medium and this is not known *a priori* for the general case. Because strain energy is stored in the medium only in the region $\Gamma \in [0, L]$, the strain energy stored during buckling associated with the stiffness of the infill is
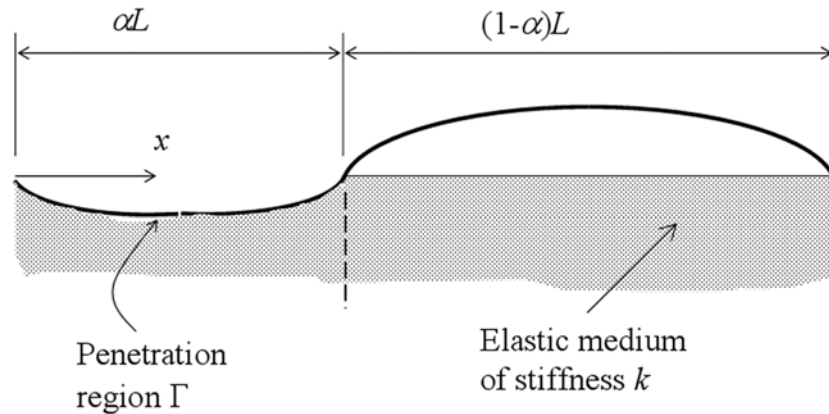
Fig. 3 Meridional cross-sectional view of local buckle in thin-walled tube and penetration region *G* in elastic infill

$$U_r = \frac{1}{2}\int_0^{\alpha L}\oint_C kw^2\,\mathrm{d}s\,\mathrm{d}x \qquad\qquad (16)$$

Prior to buckling, the strain energy stored in the tube due to axial compression is

$$U_0 = \frac{1}{2}\int_0^L\oint_C(E\varepsilon_0)\varepsilon_0 t\,\mathrm{d}s\,\mathrm{d}x = \frac{1}{2}Et\int_0^L\oint_C\varepsilon_0^2\,\mathrm{d}s\,\mathrm{d}x \qquad\qquad (17)$$

and so the total change in potential during buckling is

$$\Pi = U_b + U_m + U_r - V - U_0 \qquad\qquad (18)$$

The circumference S of an ellipse with semi-major axis a and semi-minor axis b is

$$S = \oint_C \mathrm{d}s = \oint_C\sqrt{1+\left(\frac{\mathrm{d}y}{\mathrm{d}x}\right)^2} \qquad\qquad (19)$$

which when using the change of variable defined by

$$\mathrm{d}s = \frac{1}{a}\sqrt{\frac{m}{n}}\mathrm{d}z \qquad\qquad (20)$$

with

$$m = a^4 - a^2 z^2 + b^2 z^2 \qquad\text{and}\qquad n = a^2 - z^2 \qquad\qquad (21)$$

produces

$$S = \frac{4}{a}\int_0^a\sqrt{\frac{m}{n}}\mathrm{d}z \qquad\qquad (22)$$

It is worth noting that Eq. (22) can be conveniently stated using Ramanujan's first approximation as

$$S \cong \pi[3(a+b)-\sqrt{(a+3b)(3a+b)}]\,. \qquad\qquad (23)$$

Using the contributions in Eqs. (3) and (14) to (17) in Eq. (18), the change in total potential during buckling can be written as

$$\Pi = \frac{Et^3}{6(1-v^2)a}\int_0^L\int_0^a\left(\frac{\partial^2 w}{\partial x^2}\right)^2\sqrt{\frac{m}{n}}\mathrm{d}z\mathrm{d}x + \frac{Et^3 a^3}{6(1-v^2)}\int_0^L\int_0^a\left(\frac{\partial^2 w}{\partial x^2}\right)^2\sqrt{\frac{n}{m}}\mathrm{d}z\mathrm{d}x$$

$$+ \frac{Et^3 a^7 b^4}{6(1-v^2)}\int_0^L\int_0^a\left(\frac{\partial w}{\partial z}\right)^2\frac{z^2\mathrm{d}z\mathrm{d}x}{m^3\sqrt{mn}} - \frac{Et^3 a^5 b^2}{3(1-v^2)}\int_0^L\int_0^a\frac{z}{m^2}\sqrt{\frac{n}{m}}\frac{\partial w}{\partial z}\frac{\partial^2 w}{\partial z^2}\mathrm{d}z\mathrm{d}x$$

$$+ \frac{vEt^3 a}{3(1-v^2)}\int_0^L\int_0^a\frac{\partial^2 w}{\partial x^2}\frac{\partial^2 w}{\partial z^2}\sqrt{\frac{n}{m}}\mathrm{d}z\mathrm{d}x - \frac{vEt^3 a^3 b^2}{3(1-v^2)}\int_0^L\int_0^a\frac{\partial^2 w}{\partial x^2}\frac{\partial w}{\partial z}\frac{z\mathrm{d}z\mathrm{d}x}{m^3\sqrt{m^3 n}}$$

$$+ \frac{Et^3 a}{3(1+v)}\int_0^L\int_0^a\sqrt{\frac{n}{m}}\left(\frac{\partial^2 w}{\partial x\partial z}\right)^2\mathrm{d}z\mathrm{d}x + 2Etb^2 a^7\int_0^L\int_0^a\frac{w^2\mathrm{d}z\mathrm{d}x}{\sqrt{nm^5}} + \frac{2k}{a}\int_0^{\alpha L}\int_0^a\sqrt{\frac{m}{n}}w^2\mathrm{d}z\mathrm{d}x$$

$$- \frac{2Et\varepsilon_0}{a}\int_0^L\int_0^a\sqrt{\frac{m}{n}}\left(\frac{\partial w}{\partial x}\right)^2\mathrm{d}z\mathrm{d}x\,. \qquad\qquad (24)$$

Eq. (24) is solved herein by invoking the Ritz-based solution technique described in the following.

3. One degree of freedom solution

In order to implement the Rayleigh-Ritz technique, the axial strain at elastic buckling ε_0 in Eq. (24) is determined by making the change in potential Π stationary with respect to all variations of the buckled shape w which is chosen to satisfy the kinematic boundary conditions for buckling of the elliptical cylinder. The function $^xw(x)$ defined in the in the domain $x \in [0, L]$ (or the function $^xw(\xi)$ where $\xi = x/L \in [0, 1]$) that is chosen is given by

$$^xw = {}^x\Delta \cdot \sin[\pi(\alpha - \xi)] \cdot \sin[\pi(\xi - 1)] \tag{25}$$

in which $^x\Delta$ is a deflection parameter. This function satisfies the kinematic boundary conditions that

$$^xw(\xi = 0) = {}^xw(\xi = \alpha) = {}^xw(\xi = 1) = 0 \tag{26}$$

and

$$\left(\frac{\partial w}{\partial x}\right)(\xi = 0) = -\left(\frac{\partial w}{\partial x}\right)(\xi = \alpha) \tag{27}$$

In addition, because

$$\frac{\partial^xw}{\partial x} = \left(\frac{\pi\,^x\Delta}{L}\right)\sin[\pi(\alpha + 1 - 2\xi)], \tag{28}$$

the function ^xw is periodic along the wavelength L of the cylinder and is symmetric and as

$$\left(\frac{\partial^xw}{\partial x}\right)_{\xi = 0} = \begin{cases} 0 & \alpha = 0 \\ -\pi\,^x\Delta/L & \alpha = 1/2 \end{cases} \tag{29}$$

and

$$\left(\frac{\partial^xw}{\partial x}\right)_{\xi = 1} = \begin{cases} 0 & \alpha = 0 \\ -\pi\,^x\Delta/L & \alpha = 1/2 \end{cases}, \tag{30}$$

the buckling mode is antisymmetric in the interval $\xi \in [0, 1]$. The function ^xw in Eq. (25) therefore satisfies the required kinematic boundary conditions for a tube with no infill ($k = 0$) or with a rigid infill ($k \to \infty$).

The displacement function $^sw(s)$ that is chosen in the meridional direction should also satisfy the boundary conditions. Consider a transformation of variables to $\eta = z/a \in [0, 1]$ (where $z \in [0, a]$ represents the right hand portion of the ellipse) and the function ^sw defined by

$$^sw = {}^s\Delta\left\{2\left[\frac{1 - (b/a)}{\beta^3}\right]\eta^3 - 3\left[\frac{1 - (b/a)}{\beta^2}\right]\eta^2 + 1\right\} \tag{31}$$

where $^s\Delta$ is a deflection parameter and β is the localisation parameter discussed in Section 1, so that $a\beta$ represents the projection of the buckled width in the cross-section onto the z-axis. Eq. (31) is a generic form chosen to be valid for all $a \geq b$ in modelling the meridional buckling displacement, which satisfies the boundary conditions

$$^sw(\eta = 0) = {}^s\Delta, \quad \left(\frac{\partial^sw}{\partial z}\right)(\eta = 0) = \left(\frac{\partial^sw}{\partial z}\right)(\eta = \beta) = 0 \tag{32}$$

Note that for a circular tube for which $a = b$, Eq. (31) produces $^w s = {}^s \Delta$ which represents an axisymmetric ring buckling mode and which is the same as that assumed by Bradford *et al.* (2002, 2006). In addition, when $b/a \rightarrow 0$, the oval tube tends towards a flat plate that is fixed at the edges $z = \pm a$, Eq. (31) reduces to

$$^s w = {}^s \Delta \cdot [2(\eta / \beta)^3 - 3(\eta / \beta)^2 + 1] \tag{33}$$

For a flat plate which is built-in at its edges, the plate may buckle across its entire width and so the localisation parameter is $\beta = 1$, and using this in Eq. (33) reduces the term in square brackets to the cubic interpolation function for the buckling of a plate built-in along its edges.

The axisymmetric buckling deformation $w \in \Re^2$ for the thin-walled elliptical cylinder that satisfies the boundary conditions may be obtained from the one-dimensional representations in Eqs. (25) and (31) over the domains $\xi \in \Re^1$ and $\eta \in \Re^1$ as

$$w = {}^x w \cdot {}^s w = q \cdot \left[2 \left(1 - \frac{b}{a} \right) \left(\frac{\eta}{\beta} \right)^3 - 3 \left(1 - \frac{b}{a} \right) \left(\frac{\eta}{\beta} \right)^2 + 1 \right] \cdot \sin[\pi(\alpha - \xi)] \sin[\pi(\xi - 1)] \tag{34}$$

or

$$w = q \cdot F \tag{35}$$

in which q is the maximum magnitude of the buckling displacement and the function

$$F = \mathrm{fn}(a, b, \beta, \alpha, \xi, \eta) \tag{36}$$

When Eq. (34) and its appropriate derivatives are substituted into Eq. (24), and the resulting equation that is quadratic in q is minimised by setting $\partial \Pi / \partial q = 0$ for the non-trivial buckling deformation q, the local buckling stress can be written in the form

$$\sigma_{0l} = \omega \cdot \frac{F}{\sqrt{1 - v^2} (d / 2)} t \tag{37}$$

in which the equivalent diameter

$$d = \frac{2a^2}{b} \tag{38}$$

is the diameter of the curvature of the end of the minor axis where the localised buckling initiates (Tennyson *et al.* 1971) and ω is the local buckling coefficient. The buckling coefficient is given by

$$\omega = \frac{ta}{12\sqrt{1 - v^2} L^2 \gamma} f_1 + \frac{tL^2}{12\sqrt{1 - v^2} \gamma a^3} f_2 + \frac{t\gamma^3 L^2}{12\sqrt{1 - v^2} a^3} f_3 - \frac{t\gamma L^2}{6\sqrt{1 - v^2} a^3} f_4$$

$$+ \frac{vt}{6\sqrt{1 - v^2} \gamma a} f_5 + \frac{vt\gamma}{6\sqrt{1 - v^2} a} f_6 + \frac{t}{6\gamma a} \sqrt{\frac{1 - v}{1 + v}} f_7 \frac{\gamma L^2}{ta} \sqrt{1 - v^2} f_8 + \frac{kaL}{Et^2 \gamma} \sqrt{1 - v^2} f_9 \tag{39}$$

with the terms f_1 to f_9 being given by

$$g f_1 = \int_0^1 \int_0^\beta \sqrt{\frac{\Psi}{\Gamma}} \left(\frac{\partial^2 F}{\partial \xi^2} \right)^2 d\eta d\xi, \quad g f_2 = \int_0^1 \int_0^\beta \sqrt{\frac{\Gamma^3}{\Psi^3}} \left(\frac{\partial^2 F}{\partial \eta^2} \right)^2 d\eta d\xi, \quad g f_3 = \int_0^1 \int_0^\beta \frac{\eta^2}{\sqrt{\Psi^7 \Gamma}} \left(\frac{\partial F}{\partial \eta} \right)^2 d\eta d\xi$$

$$g\,f_4 \;=\; \int\limits_{0}^{1}\int\limits_{0}^{\beta}\frac{\eta\sqrt{\Gamma}}{\sqrt{\Psi^5}}\Big(\frac{\partial^2 F}{\partial \eta^2}\Big)\Big(\frac{\partial F}{\partial \eta}\Big)\,\mathrm{d}\eta\mathrm{d}\xi, \quad g\,f_5 \;=\; \int\limits_{0}^{1}\int\limits_{0}^{\beta}\sqrt{\frac{\Gamma}{\Psi}}\Big(\frac{\partial^2 F}{\partial \xi^2}\Big)\Big(\frac{\partial^2 F}{\partial \eta^2}\Big)\,\mathrm{d}\eta\mathrm{d}\xi$$

$$g\,f_6 \;=\; \int\limits_{0}^{1}\int\limits_{0}^{\beta}\frac{\eta}{\sqrt{\Psi^3\Gamma}}\Big(\frac{\partial F}{\partial \eta}\Big)\Big(\frac{\partial^2 F}{\partial \xi^2}\Big)^2\,\mathrm{d}\eta\mathrm{d}\xi, \quad g\,f_7 \;=\; \int\limits_{0}^{1}\int\limits_{0}^{\beta}\sqrt{\frac{\Gamma}{\Psi}}\Big(\frac{\partial^2 F}{\partial \xi\partial \eta}\Big)^2\,\mathrm{d}\eta\mathrm{d}\xi$$

$$g\,f_8 \;=\; \int\limits_{0}^{1}\int\limits_{0}^{\beta}\frac{F^2}{\sqrt{\Gamma\Psi^5}}\,\mathrm{d}\eta\mathrm{d}\xi, \quad g\,f_9 \;=\; \int\limits_{0}^{1}\int\limits_{0}^{\beta}\frac{F^2\sqrt{\Psi}}{\sqrt{\Gamma}}\,\mathrm{d}\eta\mathrm{d}\xi \tag{40}$$

in which

$$g \;=\; \int\limits_{0}^{1}\int\limits_{0}^{\beta}\sqrt{\frac{\Psi}{\Gamma}}\Big(\frac{\partial F}{\partial \xi}\Big)^2\,\mathrm{d}\eta\mathrm{d}\xi, \quad \Gamma = 1-\eta^2, \quad \gamma = \frac{b}{a} \quad and \quad \Psi = \Gamma + \gamma^2\eta^2 \tag{41}$$

For the special case of a circular tube for which $a = b = r$, the axisymmetric nature of the problem dictates that $\partial(\ )\partial\eta = 0$ and so Eqs. (39) and (40) lead to

$$\omega \;=\; \frac{trf_1}{12L^2\sqrt{1-v^2}} + \frac{L^2\sqrt{1-v^2}f_5}{rt} + \frac{krL^2\sqrt{1-v^2}f_6}{Et^2} \tag{42}$$

which is the same as that derived by Bradford *et al.* (2006).

A convenient algorithm for solving the buckling problem is described in the following. The buckling coefficient w is a function of the variables β and L, which may be represented by the vector $\mathbf{r} = (\beta, L)$ so that $(\mathbf{r}, \omega) \in \mathfrak{R}^3$ represents a three-dimensional surface. The critical value of w is defined as ω_{cr} which is evaluated at $\mathbf{r} = \mathbf{r}_{cr}$, such that

$$\Big(\frac{\partial \omega}{\partial \mathbf{r}}\Big)_{r\,=\,r_{cr}} \;=\; 0\,. \tag{43}$$

For an equivalent diameter $d = 2a^2/b$, a value of $\beta = 1$ may be initially assumed and Eqs. (39) to (41) solved for small increments of L until a local minimum is found and recorded. This loop can be nested inside one in which β is decremented until the value of ω_{cr} is found to sufficient accuracy.

4. Multi degree of freedom solution

It can be seen that prescribing the assumed displacement function with one degree of freedom, as in Eq. (34), requires recourse to a numerical solution to determine the critical value of ω. To establish the accuracy of using the prescriptive one degree of freedom solution, a multi-degree of freedom solution has been developed to solve the buckling problem. For this, the assumed buckling displacement is taken as

$$w \;=\; \sum_{i=1}^{n} q_i \cdot \Big[2\Big(1-\frac{b}{a}\Big)\Big(\frac{\eta}{\beta}\Big)^3 - 3\Big(1-\frac{b}{a}\Big)\Big(\frac{\eta}{\beta}\Big)^2 + 1\Big] \cdot \sin[\pi(\alpha-\xi)]\sin[i\pi(\xi-1)] \tag{44}$$

in which q_i are the (n) buckling degrees of freedom, and for which

$$w(\xi = 0) = w(\xi = \alpha) = w(\xi = 1) = 0 \tag{45}$$

and

$$\left(\frac{\partial w}{\partial z}\right)_{\eta=0} = \left(\frac{\partial w}{\partial z}\right)_{\eta=\beta} = 0. \tag{46}$$

By rewriting Eq. (44) as

$$w = \sum_{i=1}^{n} q_i \cdot \Phi(\eta)\sin[\pi(\alpha-\xi)]\left\{\sin\left([i\pi(\xi-1)] - \frac{i}{2n}[1 + \cos(i\pi)]\sin[n\pi(\xi-1)]\right)\right\} \tag{47}$$

where $\Phi(\eta)$ is the function in Eq. (31), Eq. (44) may be expressed compactly as the scalar product

$$w = \mathbf{f}^{\mathrm{T}}\mathbf{q}, \tag{48}$$

in which $\mathbf{q} = \{q_1, q_2, , q_{n-1}\}^{\mathrm{T}}$ is the vector of buckling degrees of freedom, $\mathbf{f} = \{f_1, f_2, , f_{n-1}\}^{\mathrm{T}}$ is the vector of shape functions that is given by

$$f_i = \begin{cases} \Phi(\eta)\sin[\pi(\alpha-\xi)] \cdot \left\{\sin[i\pi(\xi-1)] - \dfrac{i}{2n}\sin[n\pi(\xi-1)]\right\} & i = 2, 4, ..., n-2 \\ \\ \Phi(\eta)\sin[\pi(\alpha-\xi)] \cdot \sin[i\pi(\xi-1)] & i = 1, 3, ..., n-2 \end{cases} \tag{49}$$

When Eqs. (48) and (49) and their appropriate derivatives are substituted into Eq. (24), the change in total potential can be written as the quadratic form in $\mathbf{q}$ as

$$\Pi = \mathbf{q}^{\mathrm{T}}\left\{\left[\frac{Et^3a}{6(1-v^2)L^3}\right]\mathbf{K}_1 + \left[\frac{Et^3L}{6(1-v^2)a^3}\right]\mathbf{K}_2 + \left[\frac{Et^3L\gamma^4}{6(1-v^2)a^3}\right]\mathbf{K}_3\right.$$

$$-\left[\frac{Et^3L\gamma^2}{3(1-v^2)a^3}\right]\mathbf{K}_4 + \left[\frac{vEt^3}{3(1-v^2)aL}\right]\mathbf{K}_5 - \left[\frac{vEt^3\gamma^2}{3(1-v^2)aL}\right]\mathbf{K}_6$$

$$\left.+\left[\frac{Et^3a}{3(1+v)L^3}\right]\mathbf{K}_7 + \left(\frac{EtL\gamma^2}{a}\right)\mathbf{K}_8 + 2kLa\mathbf{K}_9(\alpha) - \left(\frac{2Et\varepsilon_0L}{a}\right)\mathbf{K}_{10}\right\}\mathbf{q} \tag{50}$$

in which $\mathbf{K}_1, \mathbf{K}_2, ..., \mathbf{K}_{10}$ are matrices of order $(n-1)\times(n-1)$ given by

$$\mathbf{K}_1 = \int_0^1\int_0^\beta \frac{\partial^2\mathbf{f}^{\mathrm{T}}}{\partial\xi^2} \cdot \frac{\partial^2\mathbf{f}}{\partial\xi^2}\sqrt{\frac{\Psi}{\Gamma}}\,\mathrm{d}\xi\mathrm{d}\eta, \qquad \mathbf{K}_2 = \int_0^1\int_0^\beta \frac{\partial^2\mathbf{f}^{\mathrm{T}}}{\partial\eta^2} \cdot \frac{\partial^2\mathbf{f}}{\partial\eta^2}\left(\sqrt{\frac{\Psi}{\Gamma}}\right)^{3/2}\mathrm{d}\xi\mathrm{d}\eta,$$

$$\mathbf{K}_3 = \int_0^1\int_0^\beta \frac{\partial\mathbf{f}^{\mathrm{T}}}{\partial\eta} \cdot \frac{\partial\mathbf{f}}{\partial\eta}\frac{\eta^2}{\sqrt{\Psi^7\Gamma}}\,\mathrm{d}\xi\mathrm{d}\eta, \qquad \mathbf{K}_4 = \int_0^1\int_0^\beta \frac{\partial\mathbf{f}^{\mathrm{T}}}{\partial\eta} \cdot \frac{\partial^2\mathbf{f}}{\partial\eta^2}\frac{\eta}{\Psi^2}\sqrt{\frac{\Gamma}{\Psi}}\,\mathrm{d}\xi\mathrm{d}\eta,$$

$$\mathbf{K}_5 = \int_0^1\int_0^\beta \frac{\partial^2\mathbf{f}^{\mathrm{T}}}{\partial\xi^2} \cdot \frac{\partial^2\mathbf{f}}{\partial\eta^2}\frac{\Gamma}{\Psi}\,\mathrm{d}\xi\mathrm{d}\eta, \qquad \mathbf{K}_6 = \int_0^1\int_0^\beta \frac{\partial\mathbf{f}^{\mathrm{T}}}{\partial\eta} \cdot \frac{\partial^2\mathbf{f}}{\partial\xi^2}\frac{\eta^2}{\sqrt{\Psi^3\Gamma}}\,\mathrm{d}\xi\mathrm{d}\eta,$$

$$\mathbf{K}_7 = \int_0^1\int_0^\beta \frac{\partial^2\mathbf{f}^{\mathrm{T}}}{\partial\xi\partial\eta} \cdot \frac{\partial^2\mathbf{f}}{\partial\xi\partial\eta}\sqrt{\frac{\Gamma}{\Psi}}\,\mathrm{d}\xi\mathrm{d}\eta, \quad \mathbf{K}_8 = \int_0^1\int_0^\beta \mathbf{f}^{\mathrm{T}} \cdot \mathbf{f}\frac{1}{\sqrt{\Gamma\Psi^5}}\,\mathrm{d}\xi\mathrm{d}\eta,$$

$$\mathbf{K}_9 = \int_0^1\int_0^\beta \mathbf{f}^{\mathrm{T}} \cdot \mathbf{f}\sqrt{\frac{\Psi}{\Gamma}}\,\mathrm{d}\xi\mathrm{d}\eta, \qquad \mathbf{K}_{10} = \int_0^1\int_0^\beta \frac{\partial\mathbf{f}^{\mathrm{T}}}{\partial\xi} \cdot \frac{\partial\mathbf{f}}{\partial\xi}\sqrt{\frac{\Psi}{\Gamma}}\,\mathrm{d}\xi\mathrm{d}\eta \tag{51}$$

Minimising Eq. (50) with respect to **q** produces the stiffness equations

$$
\left[\left(\frac{ta}{12\sqrt{1-v^2}\, L^2 \gamma} \right) \mathbf{K}_1 + \left(\frac{tL^2}{12\sqrt{1-v^2}\, a^3 \gamma} \right) \mathbf{K}_2 + \left(\frac{tL^2 \gamma^3}{12\sqrt{1-v^2}\, a^3} \right) \mathbf{K}_3 - \left(\frac{tL^2 \gamma}{6\sqrt{1-v^2}\, a^3} \right) \mathbf{K}_4 \right.
$$

$$
+ \left(\frac{vt}{6\sqrt{1-v^2}\, a\gamma} \right) \mathbf{K}_5 + -\left(\frac{vt\gamma}{6\sqrt{1-v^2}\, a} \right) \mathbf{K}_6 + \left(\frac{t}{6a\gamma} \sqrt{\frac{1-v}{1+v}} \right) \mathbf{K}_7 - \left(\frac{L^2 \gamma \sqrt{1-v^2}}{ta} \right) \mathbf{K}_8
$$

$$
\left. + \left(\frac{kaL^2 \sqrt{1-v^2}}{Et^2 \gamma} \right) \mathbf{K}_9(\alpha) - w\mathbf{K}_{10} \right] \mathbf{q} = \mathbf{0} \tag{52}
$$

which represents an $(n\text{-}1)^{\text{th}}$ order eigenproblem of the form

$$
\mathbf{K} \cdot \mathbf{q} = \omega \mathbf{K}_{10} \cdot \mathbf{q} \tag{53}
$$

for which **K** is a function of the variables α, β and L. Eq. (53) can be solved for the eigenvalue ω in the same way as for the one-degree of freedom system, by using a suitable eigensolver, and using the results of the one-degree of freedom solution as a starting point for (β, L).

5. Illustrative examples

The solutions using $n = 1$ and 2 for an ellipse with $a = 1.5$, $b = 150$ mm (taking $v = 0.3$) are given in Table 1 for various thicknesses of the elliptical tube, and with infill an stiffness of $k \approx \infty$ ($k = 10^{14}$ N/mm^3) so that $a \approx 0$. It can be seen from this table that to an accuracy commensurate with the physical observation that the localisation takes place over a finite region defined by the parameter β, the one-degree of freedom representation is satisfactory.

Two additional cases have been considered for verification; one for an ellipse without infill ($\alpha = \frac{1}{2}$) and one for an ellipse with a rigid infill ($k \rightarrow \infty$, $\alpha = 0$) The two ellipses used had the dimensions $a = 150$ mm, $b = 100$ mm and $a = 200$ mm, $b = 100$ mm (this second ellipse was analysed using ABAQUS by Zhu and Wilkinson (2006)), and the results are shown in Tables 2 and 3 for different values of the tube thickness.

Table 1 Convergence of solution ($n = 1$ and 2) for $k \approx \infty$ ($\alpha \approx 0$)

Thickness t (mm)	Degrees of freedom n	Local buckling coefficient ω_{crit}	$(\beta, L)_{crit}$ (L in mm)
0.5	1	1.029	(0.45, 27.65)
	2	0.996	(0.46, 32.0)
1.0	1	1.042	(0.54, 39.0)
	2	1.009	(0.54, 45.1)
5.0	1	1.100	(0.795, 85.6)
	2	1.066	(0.80, 99.2)
10.0	1	1.149	(0.93, 119.4)
	2	1.114	(0.93, 138.5)

Table 2 Results for elastic buckling with $a = 1.5b = 150$ mm

t (mm)	Result	$\alpha = 0$	$\alpha = \frac{1}{2}$	ABAQUS
0.5	ω_{cr}	1.029	0.599	
	β	0.450	0.510	
	σ_{0l} (N/mm^2)	479.4	279.1	279.38
	σ_{app}/σ_{0l}	0.972	0.964	
	$2a/t$	600	600	600
	L (mm)	27.65	36.30	$195 \div 5$
1.0	ω_{cr}	1.042	0.6085	
	β	0.540	0.600	
	σ_{0l} (N/mm^2)	970.6	567.0	561.41
	σ_{app}/σ_{0l}	0.960	0.949	
	$2a/t$	300	300	
	L (mm)	39.00	51.10	$275 \div 5$
5.0	ω_{cr}	1.100	0.651	
	β	0.795	0.865	
	σ_{0l} (N/mm^2)	5,125	3,034	2879.2
	σ_{app}/σ_{0l}	0.909	0.887	
	$2a/t$	60	60	60
	L (mm)	85.6	112.2	$600 \div 5$
10.0	ω_{cr}	1.149	0.686	
	β	0.930	0.990	
	σ_{0l} (N/mm^2)	10,703	6,396	6156.8
	σ_{app}/σ_{0l}	0.871	0.841	
	$2a/t$	30	30	30
	L (mm)	119.4	156.3	$320 \div 2$

The tables also show the approximate buckling stress σ_{app} that can be determined from the closed form solution (Bradford *et al.* 2006) using an equivalent diameter of $d = 2a^2/b$ (σ_{0l} is the local buckling stress). The notation $195 \div 5$ (and similar) in the ABAQUS column of Table 2 indicates that 5 wavelengths occurred along a length of 195 mm, producing $L = 39$ mm. It can be seen from the tables that the results of the present method are consistent with the ABAQUS results, and those of Zhu and Wilkinson (2006), for a hollow elliptical tube. Disparities would be expected because the Rayleigh-Ritz solution technique uses only one harmonic function for the buckled shape lengthwise, and a single cubic function in for the projection of the meridional buckle onto the z-axis. For the case of an ellipse with a rigid infill, using a buckling stress of (Bradford *et al.* 2002, 2006)

$$\sigma_{0l,\,approx} \approx \frac{E}{\sqrt{1 - \nu^2}}\left(\frac{t}{r}\right) \tag{54}$$

that uses $\omega \approx 1$ and $r = a^2/b$ produces acceptable buckling stresses for preliminary engineering design with a rigid infill.

Table 3 Results for elastic buckling with $a = 2.0b = 200$ mm

t (mm)	Result	$\alpha = \frac{1}{2}$	Zhu and Wilkinson (2006)	ABAQUS
0.5	ω_{cr}	0.603		0.608
	β	0.470		
	σ_{0l} (N/mm^2)	158.0	-	159.26
	σ_{app}/σ_{0l}	0.958		0.950
	$2a/t$	800		800
	L (mm)	48.35		
1.0	ω_{cr}	0.607	0.620	0.621
	β	0.503		
	σ_{0l} (N/mm^2)	318.0	325	325.8
	σ_{app}/σ_{0l}	0.951	0.931	0.929
	$2a/t$	400	400	400
	L (mm)	68.3		
5.0	ω_{cr}	0.667	0.636	0.638
	β	0.800		
	σ_{0l} (N/mm^2)	1,747	1668	1671
	σ_{app}/σ_{0l}	0.8662	0.907	0.905
	$2a/t$	80	80	80
	L (mm)	148.3		
10.0	ω_{cr}	0.712	0.657	0.654
	β	0.920		
	σ_{0l} (N/mm^2)	3,729	3445	3430
	σ_{app}/σ_{0l}	0.812	0.878	0.882
	$2a/t$	40	40	40
	L (mm)	206.3		

6. Concluding remarks

This paper has described the development of an energy-based technique for determining the local buckling stress for a thin-walled elastic elliptical tube subjected to uniform axial compression, and which contains an elastic infill that inhibits the formation of a local buckle in the wall of the thin elliptical tube. The formulation is founded on a statement of the change of total potential from the prebuckled to the buckled configuration. Minimisation of this change in potential then leads to the familiar eigenvalue representation for the buckling load.

The representation of the displacement function in the meridional and tangential directions satisfied all of the kinematic boundary conditions; the tangential displacement function used the physically observed concept of localisation of the buckle in the region of lowest curvature of the ellipse. This representation was used to derive a one degree of freedom solution for the buckling stress in analytic form, but which needs a simple numerical technique to extract the lowest local buckling solution. It as also used to derive a multi degree of freedom solution for the buckling coefficient using stiffness matrices. The one degree of freedom solution is accurate in comparison with the stiffness matrix solution, and was shown to be accurate compared with an ABAQUS modelling for a hollow tube.

Acknowledgement

References

ABAQUS Analysis User's Manual (2006), Abaqus Inc., Pawtucket, Rhode Island.

Black, C.J., Markis, N. and Aitken, I.D. (2004), "Component testing, seismic evaluation and characterization of buckling-restrained braces", *Journal of Structural Engineering, ASCE*, **130**(6), 880-894.

Bortolotti, E., Jaspart, J.E., Pietrapertose, C., Nicaud, G., Petitjean, P.D. and Grimault, J.P. (2003), "Testing and modelling of welded joints between elliptical hollow sections", *Proceedings of 10th International Conference on Tubular Structures*, Madrid.

Bradford, M.A. and Roufegarinejad, A. (2006), "Elastic buckling of thin circular tubes with an elastic infill under uniform compression", *Proceedings of 11th International Conference on Tubular Structures*, Quebec, 359-364.

Bradford, M.A. and Vrcelj, Z. (2004), "Elastic local buckling of thin-walled square tubes containing an elastic infill", *Proceedings of 4th International Conference on Thin-Walled Structures*, Loughborough, UK, 893-900.

Bradford, M.A., Loh, H.Y. and Uy, B. (2002), "Slenderness limits for circular steel tubes", *Journal of Constructional Steel Research*, **58**(2), 243-252.

Bradford, M.A., Roufegarinejad, A. and Vrcelj, Z. (2006), "Elastic buckling of thin-walled circular tubes containing an elastic infill", *International Journal of Structural Stability and Dynamics*, **6**(4), 457-474.

Chan, T.M. and Gardener, L. (2006), "Experimental and numerical studies of elliptical hollow sections under axial compression and bending", *Proceedings of 11th International Conference on Tubular Structures*, Quebec, 163-170.

Gardner, L. and Chan, T.M. (2006), "Cross-section classification of elliptical hollow sections", *Proceedings of 11th International Conference on Tubular Structures*, Quebec, 171-177.

Guillow, S.R., Lu, G. and Grzebieta, R.H. (2001), "Quasi-static axial compression of thin-walled circular aluminium tubes", *International Journal of Mechanical Sciences*, **43**(9), 2103-2123.

Hutchinson, J.W. (1968), "Buckling and initial post-buckling behavior of oval cylindrical shells under axial compression", *Journal of Applied Mechanics, ASME*, **35**, 66-72.

Hyer, M.W. and Vogl, G.A. (2001), "Response of elliptical composite cylinders to a spatially uniform temperature change", *Composite Structures*, **51**(2), 169-179.

Kempner, J. (1962), "Some results on buckling and post buckling of cylindrical shells", *NASA* TN D-1510.

Maguerre, K. (1951), "Stability of cylindrical shells of variable curvature", *NACA* TM 1302.

Mahadi, E., Hamouda, A.S.M., Mokhtar, A.S. and Majid, D.L. (2005), "Many aspects to improve damage tolerance of collapsible composite energy absorber devices", *Composite Structures*, **67**(2), 175-187.

Meyers, C.A. and Hyer, M.W. (1999), "Response of elliptical composite cylinders to axial compression loading", *Mechanics of Composite Materials and Structures*, **6**(2), 169-194.

Pinna, B. and Ronalds, B.F. (2000), "Hydrostatic buckling of shells with various boundary conditions", *Journal of Constructional Steel Research*, **56**(1), 1-16.

Smith, S.T., Bradford, M.A. and Oehlers, D.J. (2000), "Unilateral buckling of elastically restrained rectangular mild steel plates", *Computational Mechanics*, **26** (4), 317-324.

Teng, J.G. (1996), "Buckling of thin shells: recent advances and trends", *Applied Mechanics Reviews, ASME*, **123**, 1622-1630.

Tennyson, R.C, Booton, M. and Caswell, R.D. (1971), "Buckling of imperfect elliptical cylindrical shells under axial compression", *AIAA Journal*, **9**(2), 250-255.

Timoshenko, S.P. and Goodier, J.N. (1970), *Theory of Elastic Stability*, 3rd edn., McGraw-Hill, New York.

Uy, B. (2001), "Strength of short concrete filled high strength steel box columns", *Journal of Constructional Steel Research*, **57**(2), 113-134.

Zhu, Y. and Wilkinson, T. (2006), "Finite element analysis of structural steel elliptical hollow sections in pure compression", *Proceedings of 11th International Conference on Tubular Structures*, Quebec.